Ion association effects and phase separation in poly(propylene oxide) modified poly(dimethylsiloxane) complexed with triflate salts

P. Jacobsson, I. Albinsson, B.-E. Mellander and J. R. Stevens*
Department of Physics, Chalmers University of Technology, S-41296 Göteborg, Sweden
(Received 1 May 1991; accepted 2 October 1991)

Phase separation is observed in poly(propylene oxide) modified poly(dimethylsiloxane) (PPO–PDMS) with excess poly(propylene oxide) (PPO) when salts of MCF_3SO_3 (M = Li, Na) are added. The same behaviour is inferred for KCF_3SO_3. The solutions above and below the boundary layer have been studied by Raman spectroscopy and in particular by examining the non-degenerate, symmetric stretch (A_1, SO_3) Raman mode of the $CF_3SO_3^-$ anion. The upper part is siloxane rich; salt is present on both sides of the boundary layer with a much lower concentration in the upper part. The formation of the boundary layer is attributed to an increasing difference in surface tension between the PPO/salt/PPO–PDMS complexes and the separate PPO, PPO–PDMS components. The boundary layer moves up with increase in concentration. The number of 'free' ions decreases and ion association increases with increase in temperature. There is evidence of contact ion pairs, triplets and aggregates. Values of conductivity are quoted for 293 K.

(Keywords: $LiCF_3SO_3$; $NaCF_3SO_3$; KCF_3SO_3; poly(propylene oxide); poly(dimethylsiloxane); polymer electrolyte; Raman spectroscopy)

INTRODUCTION

Ethylene oxide (EO) and propylene oxide (PO) monomers incorporated into short chains as homopolymers or copolymers (with terminations such as OH, CH_3, etc.) can be complexed with alkali metal salts. Such polyether–salt systems are useful models of polymer electrolytes. Their practical use in electrochromic devices, batteries and fuel cells is, however, limited since these systems are hygroscopic and the poly(ethylene oxide)–salt system crystallizes below about 60°C.

Considerable effort has gone into forming networks of polyether with flexible chains by blending, grafting and cross-linking so that crystallization is prevented and/or the ether oxygen sites are shielded from water while overall flexibility is retained or enhanced[1–7]. Examples of such systems are polyalkyl modified poly(dimethylsiloxanes) (PDMS)[2–3]. We have completed a study of ionic conductivity in poly(ethylene oxide) (PEO) modified PDMS complexed with MCF_3SO_3 (M = Li, Na, K) which showed that crystallinity is prevented and that ionic conductivities up to 10^{-4} S cm^{-1} at room temperature are acheivable[8]. Subsequently a study of poly(propylene oxide) (PPO) modified PDMS (PPO–PDMS) was initiated. However, as we dissolved $LiCF_3SO_3$ into the PPO–PDMS solvent we observed two distinct but clear regions (with different refractive indices). The boundary layer moves up with increase in concentration of the salt and for a concentration of 6 mol% $LiCF_3SO_3$ the boundary layer moves down with increase in temperature.

This paper reports on ionic effects in these two regions using Raman spectroscopy to study the behaviour of the non-degenerate symmetric stretch (A_1, SO_3) modes in the $CF_3SO_3^-$ anion as a function of temperature.

EXPERIMENTAL

The PPO–PDMS sample was obtained from Union Carbide. It was monodisperse with a molecular weight of 3000 and a viscosity of 175 mm^2 s^{-1} at 25°C. In the polymerization 30% additional PO was added to the silane (SiH) to ensure the required Si–C grafting. The synthesis and properties of these polymers are discussed by Khan *et al.*[3]. Under a vacuum better than 1.333×10^{-3} Pa these liquids were stringently freeze dried using freeze–pump–thaw cycles. While still under vacuum the samples were transferred to an argon atmosphere where newly purchased $LiCF_3SO_3$, $NaCF_3SO_3$ or KCF_3SO_3 (Aldrich) was dissolved directly into the liquids without a volatile solvent intermediary. The salts were predried in a vacuum oven at 125°C for 24 h. The doped samples were stored in a dry atmosphere. Without this stringent drying procedure it is very much more difficult, if not impossible, to dissolve the salts in the temperature range of 70–90°C used here. Using *FT*i.r. and Raman spectroscopy we have looked for the water bending mode at 1635 cm^{-1} or the stretch mode in the region 3600–3700 cm^{-1}. There is no

*Permanent address: Department of Physics, University of Guelph Guelph, Ontario, N1G 2W1, Canada

0032-3861/92/132778-06

a

PPO-PDMS

$M_w = 3000$

X = 7

Y = 3, N = 12

b

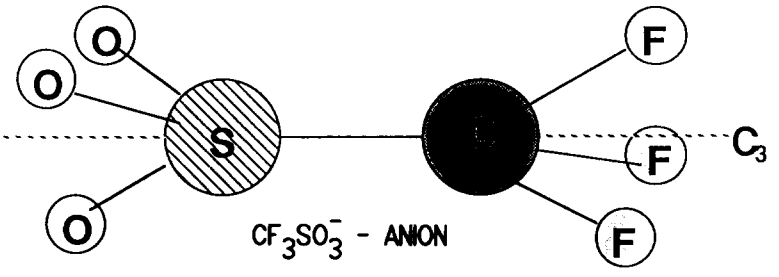

Figure 1 Schematic of (a) PPO–PDMS copolymer and (b) the $CF_3SO_3^-$ anion

evidence of water or OH. In the region 3600–3700 cm^{-1} the background was about 2 counts s^{-1} cm in the Raman spectra. The nearest polymer modes (2900–3000 cm^{-1}) had an intensity of 1000 times this value. Further, using ^1H n.m.r. we have not been able to detect the presence of water. We suggest our samples have a maximum of 0.01% water by weight.

A schematic of the PPO–PDMS system used here is shown in *Figure 1a* and a schematic of the $CF_3SO_3^-$ anion is shown in *Figure 1b*. In order to get approximately an equal amount of material in the upper and lower regions of the PPO–PDMS/salt solutions, 6 mol% $LiCF_3SO_3$ and 4 mol% $NaCF_3SO_3$ were used. As mentioned above, both regions of the lithium system were clear. The upper region of the sodium system was clear, the lower cloudy. KCF_3SO_3 was very difficult to dissolve in PPO–PDMS; no boundary layer was observed. Our final PPO–PDMS/KCF_3SO_3 had a salt concentration of 0.5 mol%. Even then there were a few undissolved crystals at the bottom of the cell.

The experimental set-up for Raman spectroscopy includes an argon ion laser operating at 488 nm with 500 mW output power, a Spex double monochromator (model 1403) with 1800 lines mm^{-1} holographic gratings and a liquid nitrogen cooled charge coupled device (CCD). The CCD has a low signal-to-noise ratio and gives a 'readout' resolution of about 0.2 cm^{-1} with rapid recordings. The overall instrumental resolution, mainly restricted by the slitwidths, was set to give a value of 1 cm^{-1}. At all temperatures a continuous flow cryostat (Oxford CF1204) with a stability better than 0.1 K was used. In order to examine Raman scattered light from the two regions separately, two-dimensional images from the CCD were used. These images clearly showed the two regions and the boundary layer between them. It was then easy to align the experimental set-up so that light from one region at a time was examined.

The bandshape of the non-degenerate symmetric stretch (A_1, SO_3) mode was analysed in detail. The Raman spectra of pure PPO–PDMS were measured and subtracted from the spectra of the salt solutions at every temperature. The remaining Raman profiles were then deconvoluted from the instrumental function using a numerical method[9]. We then tried to fit various combinations of Lorentzian and Gaussian shaped peaks to the deconvoluted spectra. It was found that the best fit was obtained with the combination of three peaks, Lorentzian, Gaussian and Lorentzian (in order of increasing frequency).

The complex impedance was measured using a computer controlled HP4274A LCR-meter over a frequency range of 100 Hz to 100 kHz with an applied signal of 20 mV. Stainless steel electrodes were used. The sample temperature was measured using a Platinel II thermocouple. The complex impedance measurements were performed in a dry atmosphere.

RESULTS

Figure 2 shows the Raman spectrum from 100 to 1100 cm^{-1} at 300 K for the upper and lower parts of the PPO–PDMS/$LiCF_3SO_3$ system detected with a photomultiplier tube. The internal vibration modes of the $CF_3SO_3^-$ anion are marked by an asterisk and are identified as by Schantz *et al.*[10]. The broad band centred at about 500 cm^{-1} (labelled 1) is due to Si–C stretching vibration[11]. These occur in the 500–900 cm^{-1} region of the spectrum and their frequencies are considerably influenced by the nature of substituted groups; the frequencies go down as the length of the substituent (side) groups increases. The PPO carbon–hydrogen stretching vibrations in the 800–900 cm^{-1} region of the spectrum are labelled 2. This identification was confirmed by comparison with the spectrum for pure PPG. We

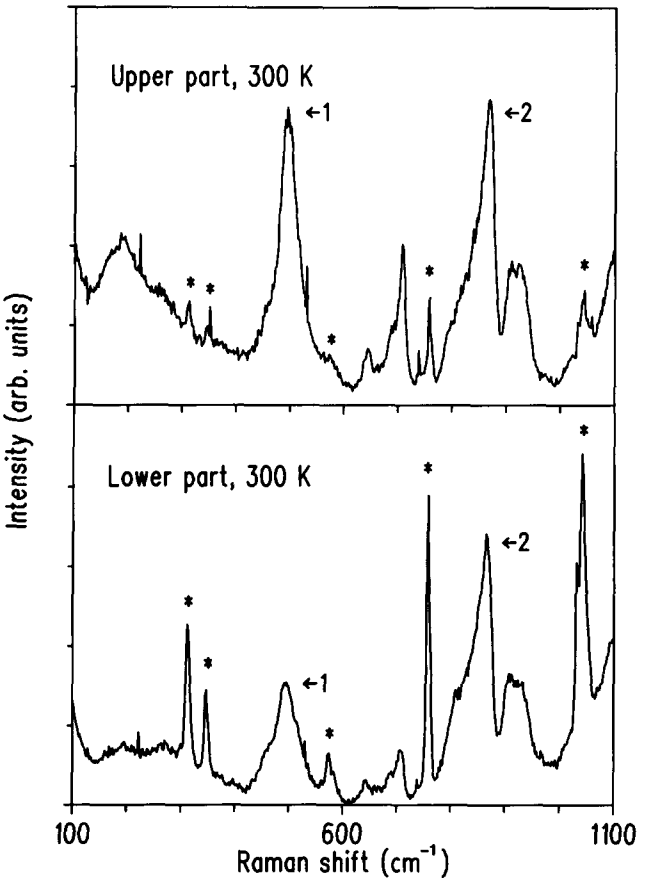

Figure 2 Raman spectra of the upper and lower parts of the PPO–PDMS/$LiCF_3SO_3$ complex at 300 K. Peaks for the Si–C stretching vibration (1) and for the PPO carbon–hydrogen stretching vibrations (2) are shown. The internal vibration modes of the $CF_3SO_3^-$ anion are marked with an asterisk

conclude from *Figure 2* that there is salt in both the upper and lower portions of the clear but separated liquid. Also, since the ratio of the intensities of the bands 1 and 2 in the upper part is much greater than the ratio in the lower part we conclude that the upper part is siloxane rich.

Figure 3 shows the deconvoluted CCD spectra for PPO–PDMS/$LiCF_3SO_3$ at 250 K for the (A_1, SO_3) mode with the spectra for pure PPO–PDMS subtracted. The fitted results with the three underlying peaks are also shown. The intensity of light scattered from the lower part in this spectral region is about six times the intensity in the upper part. Based upon previous experience with $LiCF_3SO_3$ dissolved in acetone and in poly(propylene glycol) (PPG)[12] we identify the Lorentzian centred at 1032.7 cm^{-1} with the 'free' $CF_3SO_3^-$ anion, the Gaussian centred at 1042.5 cm^{-1} with $Li^+CF_3SO_3^-$ contact ion pairs and with the $(CF_3SO_3^-)_2Li^+$ triplet-1, and the Lorentzian centred at 1053 cm^{-1} with the $(Li^+)_2CF_3SO_3^-$ triplet-2. There is no evidence of higher aggregates. *Figure 4* shows the CCD spectra for a temperature of 400 K. The frequencies of the Lorentzian, Gaussian and Lorentzian peaks have systematically shifted down to, respectively, 1031.7, 1040.6 and 1050.3 cm^{-1}.

In *Figure 5* we compare the (A_1, SO_3) profiles for light scattered from the lower part at 300 K for $LiCF_3SO_3$ (A), $NaCF_3SO_3$ (B) and KCF_3SO_3 (C) in PPO–PDMS. The baselines have been displaced for a clearer presentation. The 'free' anion peaks at 1032.6 cm^{-1} (A), 1032.4 cm^{-1} (B) and 1032.2 cm^{-1} (C) indicate a very slight influence of the cations on the $CF_3SO_3^-$ anion through the PPO–PDMS solvent which separates them. This small cation effect is the reason for 'free' being within quotation marks. The effective electric field around these cations decreases as $Li^+ > Na^+ > K^+$. From conductivity measurements, discussed below, we estimate the concentration of the lithium salt in the lower part to be $\simeq$8 mol%, the sodium salt to be $\simeq$6 mol% and the potassium salt to be $\simeq$0.5 mol%. The contact pair, triplet-1 peaks occur at 1042.2 cm^{-1} (A), 1037.6 cm^{-1} (B) and 1033.6 cm^{-1} (C) indicating a dramatic cation effect and supporting our identification. The triplet-2 peaks occur at 1052.1 cm^{-1} (A) and 1045.9 cm^{-1} (B) showing the effect of two cations on the anion; much less for $(Na^+)_2CF_3SO_3^-$ than for $(Li^+)_2CF_3SO_3^-$. The Gaussian line centred at 1058 cm^{-1} (B) is identified as an aggregation of ions. (A backscatter Raman measurement was made on a $NaCF_3SO_3$ pellet and showed a narrower but similar profile centred at about the same frequency[13].) We have previously[12] identified the ion aggregation for $LiCF_3SO_3$ in acetone to be centred at about 1076 cm^{-1}. In spectrum C of *Figure 5* we resolve a third peak at 1045 cm^{-1} which we attribute to an aggregation of ions including the triplet-2 which we are not able to resolve. The frequencies for the deconvoluted spectral components for light scattered at 300 K for lithium and sodium systems from the upper part were the same for the 'free' anion peaks and within 0.5 cm^{-1} for the other two peaks under the main profile. As mentioned above, there was no upper part for the PPO–PDMS/KCF_3SO_3 system.

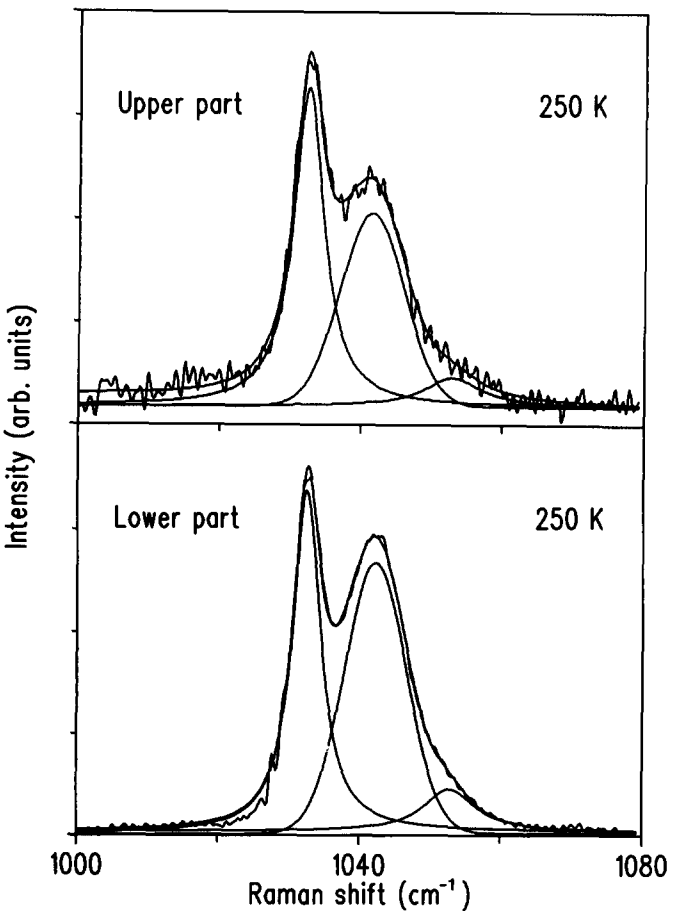

Figure 3 Deconvoluted Raman (A_1, SO_3) modes for the upper and lower parts of the PPO–PDMS/$LiCF_3SO_3$ complex at 250 K showing the underlying fitted profiles

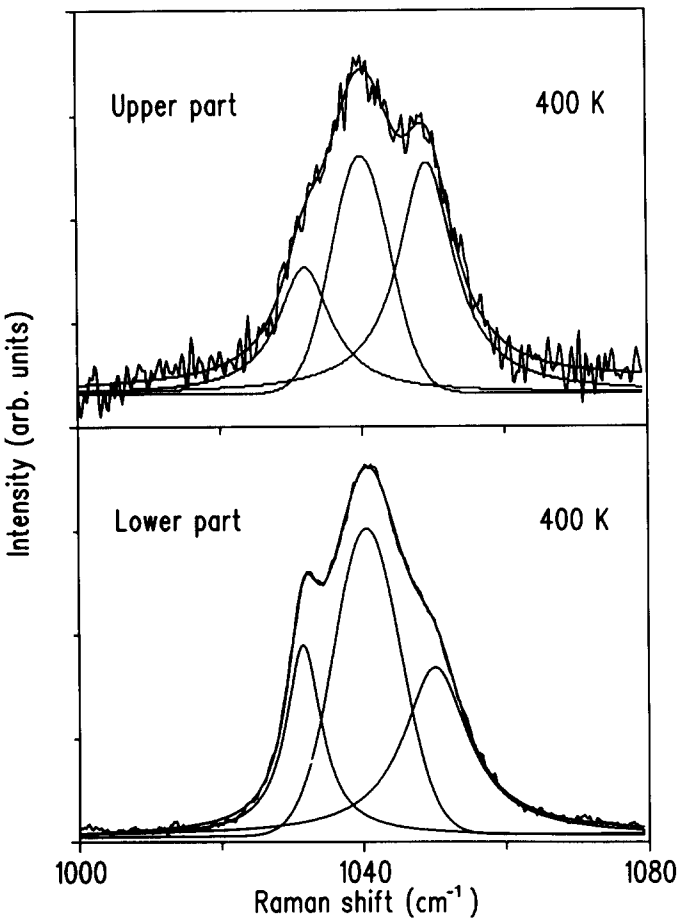

Figure 4 Deconvoluted Raman (A_1, SO_3) modes for the upper and lower parts of the PPO–PDMS/$LiCF_3SO_3$ complex at 400 K showing the underlying fitted profiles

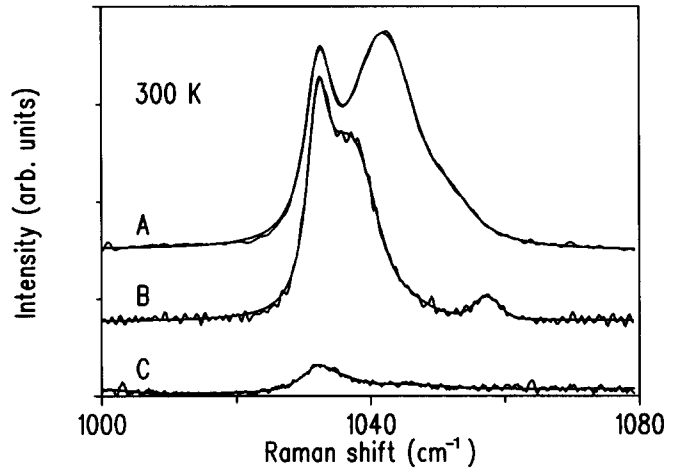

Figure 5 Deconvoluted Raman (A_1, SO_3) modes for the lower parts of the PPO–PDMS/$LiCF_3SO_3$ (A), the PPO–PDMS/$NaCF_3SO_3$ (B) and the PPO–PDMS/KCF_3SO_3 (C) complexes. The baselines have been displaced for clearer presentation. All spectra are to the same scale

The relative Raman intensity for each of the spectral components is proportional to the number of the ionic species which scattered light to produce that component. In *Figures 6* and *7* the relative Raman intensities are plotted against temperature for the PPO–PDMS/$LiCF_3SO_3$ complex (*Figure 6*) and for the PPO–PDMS/$NaCF_3SO_3$ complex (*Figure 7*). The trends are generally the same in the upper and lower parts. That is, with increase in temperature the number of 'free' ions decreases, the number of contact ion pairs and triplets-1 remains about the same and the number of triplets-2 increases; ion association increases with increase in temperature.

DISCUSSION

The formation of the boundary layer in the PPO–PDMS/$LiCF_3SO_3$ solution and in the PPO–PDMS/$NaCF_3SO_3$ solution is related to the following facts. There are two types of PO chains; those attached through Si–C bondage to the siloxane chain and those that are isolated: for every 10 PO units in the former there are three PO units in the latter. Before the salt is added the PPO–PDMS chains are miscible with the PPO. At room temperature the surface tension of PPG chains (molecular weights $\simeq$2000–3000) is 32 mN m^{-1} and for PDMS (molecular weight $\simeq$700) it is 19 mN m^{-1}; both values of the surface tension decrease with increasing temperature[14]. The interfacial tension between PPO and PDMS is 9 mN m^{-1} and decreases with increasing temperature indicating an upper consolute curve and an upper critical solution temperature. On adding the $LiCF_3SO_3$ salt a boundary layer is formed which moves upward with increasing salt concentration. The upper part is siloxane rich and there is evidence of salt on both sides of the boundary layer with a higher concentration in the lower part. The boundary layer is more clearly established with the lithium salt than

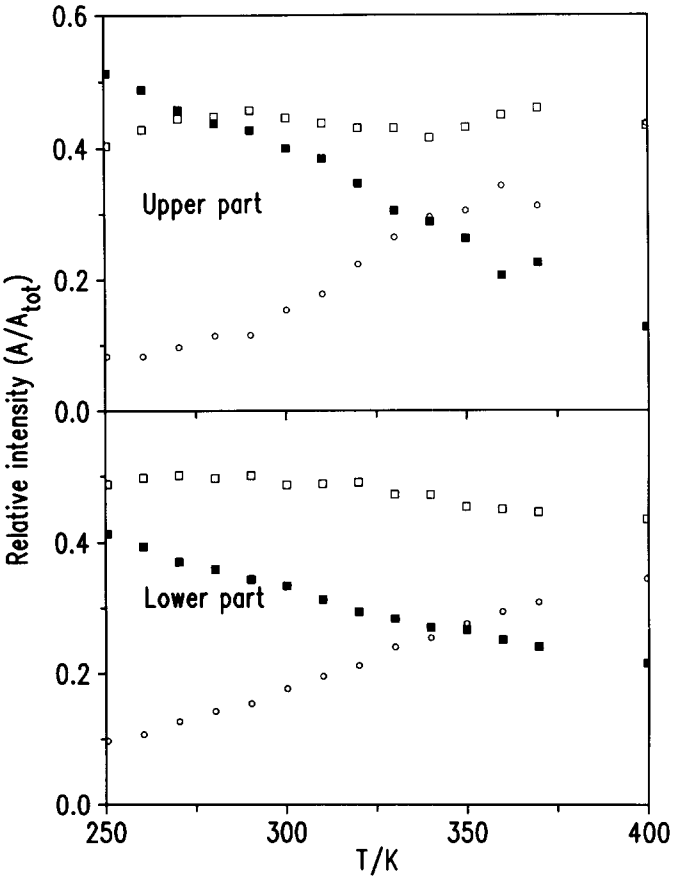

Figure 6 Relative Raman intensities of the fitted profiles for the (A_1, SO_3) modes for the upper and lower parts of the PPO–PDMS/$LiCF_3SO_3$ complex plotted against temperature. Shown are 'free' anions (■), contact ion pairs and triplets-1 (□) and triplets-2 (○)

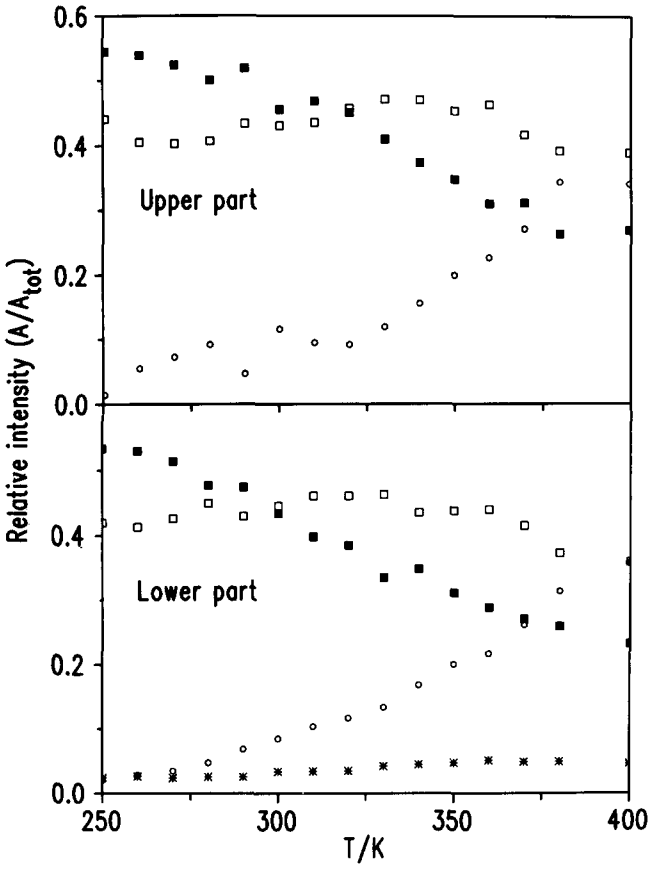

Figure 7 Relative Raman intensities of the fitted profiles for the (A_1, SO_3) modes for the upper and lower parts of the PPO–PDMS/$NaCF_3SO_3$ complex plotted against temperature. Shown are 'free' anions (■), contact ion pairs and triplets-1 (□), triplets-2 (○) and aggregates (*)

with the sodium salt, where a lower salt concentration produces the same separation. We were not able to form a boundary layer in the PPO–PDMS/KCF_3SO_3 complex. We suspect that if it occurs at all it is at very low concentration and we intend to study this further.

When the salt is dissolved in the PPO–PDMS plus PPO system it first dissociates; the cations then solvate through coordination with ether oxygen atoms in the PPO forming transient cross-links and the $CF_3SO_3^-$ anions locate in the polymer matrix and are not solvated. From the behaviour of these cations in crown ethers, we would expect that, on average, Li^+ coordinates with four ether oxygens, Na^+ with five and K^+ with six.

From the above facts we suggest that those ungrafted PPO chains which are transiently cross-linked with each other and with the PPO–PDMS copolymers move to the lower region; their surface tension, larger than that of the PPO–PDMS copolymer to begin with, increases even further as the salt is added. We suggest that this is the main effect which produces the boundary layer. As the salt concentration increases more groups of segments diffuse down and the boundary layer moves upward as we have observed. For a given concentration of salt (6 mol% $LiCF_3SO_3$ in PPO–PDMS) the boundary layer moves down with increase in temperature. Ions are released from the ether oxygen sites[15] and ion association increases; some PPO chains are released. Since the Na^+ cation ties up more PPO segments, a lower concentration is required to produce a boundary layer at the same position as that for the Li^+ cation. This trend should continue for the K^+ cation where we infer that a very low concentration of KCF_3SO_3 is required.

We have previously studied[6] the ability of these salts to act as compatibilizing agents; Li > Na > K. This accounts for the fact that the lower part of the PPO–PDMS/$LiCF_3SO_3$ is clear and the lower part of PPO–PDMS/$NaCF_3SO_3$ is cloudy.

The number of 'free' ions decreases and ion association increases with increase in temperature (*Figure 6* and 7). In *Figure 6* the relative Raman intensity of the 'free' anion profile for the lower part of the PPO–PDMS/$LiCF_3SO_3$ solution decreases from 0.41 at 250 K to 0.25 at 350 K. This decrease is similar to that observed[12] for PPG 4000/$LiCF_3SO_3$ with 6 mol% salt (0.41 at 250 K to 0.28 at 350 K).

However, there is a slight difference between the two systems when the relative intensities of the contact ion pair and triplet profiles are considered; more triplets are formed in the PPO–PDMS/$LiCF_3SO_3$ complex with increase in temperature. Any differences should be attributable to the increased flexibility of the shorter PPO side chains in PPO–PDMS[12], to the fact that the PPO units are C_4H_9 capped compared to the hydroxyl capping of the much longer PPG 4000 chain ($\simeq$3 mol% OH groups), and to any difference in salt concentration. With respect to the last point it is difficult to estimate the salt concentration in the two parts of the PPO–PDMS/$LiCF_3SO_3$ solution. We were able to extract the top part and measure its conductivity, (2.0×10^{-7} S cm^{-1} at 293 K), and then extract the lower part which had a conductivity of 2.2×10^{-6} S cm^{-1} at 293 K. We then prepared various concentrations between 1 and 10 mol% $LiCF_3SO_3$ and saw that the boundary layer moved upwards; both the 1 mol% and the 10 mol% solutions were clear with no boundary layer. We were then easily able to measure the conductivity of these two extremes and by comparing conductivities inferred that the concentration in the upper part is about 1 mol% and in the lower part about 8 mol%.

According to these and previous results[16] the conductivity should be greater in the PPO–PDMS/$LiCF_3SO_3$ complex than in the PPG 4000/$LiCF_3SO_3$ complex. At 8 mol% the ionic conductivity in the latter complex[16] is 7.3×10^{-7} S cm^{-1} at 293 K compared with 2.2×10^{-6} S cm^{-1} for the 8 mol% PPO–PDMS/$LiCF_3SO_3$ complex. The upper part of the PPO–PDMS/$NaCF_3SO_3$ complex had a conductivity of $\simeq 1.6 \times 10^{-7}$ S cm^{-1} at 293 K with an estimated salt concentration of $\simeq$0.5 mol%. For the PPO–PDMS/$NaCF_3SO_3$ complex the boundary layer had moved to the top at 6 mol% salt concentration.

CONCLUSIONS

We have observed a phase separation in a PPO–PDMS/MCF_3SO_3 complex (M = Li, Na) which contains excess PPO chains. The upper parts are siloxane rich; salt is present in both parts although by about a factor of eight times less in the upper part. The formation of the boundary layer is attributed to an increasing difference in surface tension between the PPO/salt/PPO–PDMS complexes and the separate PPO, PPO–PDMS components. In the PPO–PDMS/$LiCF_3SO_3$ solution both parts are clear, whereas in the PPO–PDMS/$NaCF_3SO_3$ solution the lower part is cloudy. This is evidence of the better

compatibilizing ability of the $LiCF_3SO_3$ salt compared to the $NaCF_3SO_3$ salt.

A study of the non-degenerate (A_1, SO_3) Raman mode of light scattered from the upper and lower parts of PPO–PDMS/MCF_3SO_3 (M = Li, Na) shows a splitting into three profiles, with an additional high frequency profile for the lower part of the $NaCF_3SO_3$ solution. We also infer four profiles for the PPO–PDMS/KCF_3SO_3 system. The lowest frequency (Lorentzian) profile is attributed to 'free' anions. There is very slight cation dependence which is attributed to coulombic effects through the separating solvent; $Li^+ > Na^+ > K^+$. The next highest frequency (Gaussian) profile is attributed to contact ion pairs and $(CF_3SO_3^-)_2Li^+$ triplets; here there is a pronounced cation dependence. $(Li^+)_2CF_3SO_3^-$ triplets produce the next highest frequency (Lorentzian) profile, with an even greater cation dependence than for the contact ion pair–triplet profile. The highest frequency profile found in the PPO–PDMS/MCF_3SO_3 systems (M = Na, K) is due to aggregates; here we have the largest cation dependence. Comparison with PPG/$LiCF_3SO_3$, in which the chains are hydroxyl capped, indicates little effect, if any, of the C_4H_9 capping in the PPO–PDMS/$LiCF_3SO_3$ complex on the 'free' ion population and its variation with temperature. 'Free' ions decrease and ion association increases with increase in temperature. However, due to the increased flexibility of the PPO chains in the PPO–PDMS copolymer the ionic conductivity is greater in the PPO–PDMS/$LiCF_3SO_3$ complex than in the PPG 4000/$LiCF_3SO_3$ complex.

ACKNOWLEDGEMENTS

The authors express their appreciation to Professor Lena Torell for her hospitality and the use of her excellent laboratory facilities. They also acknowledge financial support from the Swedish Natural Science Research Council. J.R.S. acknowledges financial support from the Swedish Board for Technical Development for a visiting professorship.

REFERENCES

1 Watanabe, M. and Ogata, N. in 'Polymer Electrolyte Reviews I' (Eds J. R. MacCallum and C. A. Vincent), Elsevier Applied Science, London, 1987, p. 39; Watanabe, M. and Ogata, N. *Br. Polym. J.* 1988, **20**, 181
2 Spindler, R. and Shriver, D. F. *J. Am. Chem. Soc.* 1988, **110**, 3036
3 Khan, I. M., Yuan, Y., Fish, D., Wu, E. and Smid. J. *Macromolecules* 1988, **21**, 2684
4 Zhou, G., Khan, I. M. and Smid, J. *Polym. Commun.* 1989, **30**, 52
5 Ballard, D. G. H., Cheshire, P., Mann, T. S. and Przeworski, T. E. *Macromolecules* 1990, **23**, 1257
6 Mani, T. and Stevens, J. R. *Polymer* 1992, **33**, 834
7 Abraham, K. M. and Alamgir, M. *J. Electrochem. Soc.* 1990, **137**, 1657
8 Albinsson, I., Mellander, B.-E. and Stevens, J. R. *Polymer* 1991, **32**, 2712
9 Jansson, P. A. in 'Deconvolution with Application in Spectroscopy', Academic Press, New York, 1984, pp. 102–111
10 Schantz, S., Sandahl, J., Börjesson, L., Torell, L. M. and Stevens, J. R. *Solid State Ionics* 1988, **28–30**, 1047
11 Bellamy, L. J. 'The Infrared Spectra of Complex Molecules', Vol. 1, 3rd Edn, Chapman and Hall, London, 1975, p. 375
12 Stevens, J. R. and Jacobsson, P. *Can. J. Chem.* 1991, **69**, 1980
13 Kakihana, M., Schantz, S., Stevens, J. R. and Torell, L. M. *Solid State Ionics* 1990, **40/41**, 641
14 Brandrup, J. and Immergut, E. H. (Eds), 'Polymer Handbook' Wiley, New York, 1989, p. VI/411
15 Schantz, S., Torell, L. M. and Stevens, J. R. *J. Chem. Phys.* 1991, **94**, 6862
16 Albinsson, I., Mellander, B.-E. and Stevens, J. R. *J. Chem. Phys.* 1992, **96**, 681